Available online at www.sciencedirect.com
ScienceDirect
Journal of Power Sources 167 (2007) 520–523
JOURNAL OF POWER SOURCES
www.elsevier.com/locate/jpowsour

Short communication

Electrochemical properties of Si–Zn–C composite as an anode material for lithium-ion batteries

Sukeun Yoon [a], Cheol-Min Park [a], Hansu Kim [b], Hun-Joon Sohn [a,*]

[a] *School of Materials Science and Engineering, Research Center for Energy Conversion and Storage, Seoul National University, Seoul 151-742, Republic of Korea*
[b] *Materials Laboratory, Samsung Advanced Institute of Technology, Yongin-si, Gyeounggi-do 449-712, Republic of Korea*

Received 2 November 2006; accepted 31 January 2007
Available online 1 March 2007

Abstract

A Si–Zn–C composite material is prepared by mechanical ball-milling and investigated as an anode material for lithium-ion batteries. Electrochemical tests show that the first charge and discharge capacities are approximately 852 and 607 mAh g^{-1}, respectively, and that 91% of the initial discharge capacity of 607 mAh g^{-1} can be maintained for up to 40 cycles. This improved cycling performance is attributed to the use of the third element Zn. Li_2ZnSi is partially formed at the interface between Si and Zn and graphite to provide superior cycling performance compared with that of the binary system.

Keywords: Lithium-ion batteries; Anode materials; Si composites; Zintl phases

1. Introduction

The development of electronic devices has led to increasing demands for batteries with high specific energy. In this regard, considerable effort has been made to use Al, Si and Sn based systems as alternative anodes for lithium-ion batteries. In particular, the use of silicon alloys has attracted much attention, because of their high theoretical specific capacity, e.g., 3580 mAh g^{-1} in the case of $Li_{15}Si_4$. Their commercial usage has been hindered, however, on account of their low electrical conductivity and the capacity fading caused by the large volume change (323%) during the charge–discharge reaction [1,2]. In order to solve these problems, many Si composite materials have been developed [3–12]. Among these, carbon-coated Si composite materials composed of active and inactive phases have been found [5–8] to exhibit a high capacity and improved cycleability, due to buffering of the mechanical stress generated during cycling and also enhanced electrical connection with the current-collector induced by the conducting inactive phase and coated carbon. Nevertheless, although the use of inactive phases increases the electrical contact and minimizes the mechanical stress, it also causes a loss of specific energy.

Recently, studies [13,14] of several Si–M binary systems (M: Sn, Ag, Zn) prepared by sputtering showed that all of the components react with lithium without any loss of specific energy. Also, these amorphous samples had high specific capacities and low irreversible capacities.

The approach in this study is to enhance the capability of Si for reversible lithium storage through a synergistic effect of Zn and graphite. A Si–Zn–C composite material is prepared by the mechanical ball-milling of Si, Zn and Mesocarbon microbeads (MCMB). The electrochemical characteristics of this composite material when used as an anode material for lithium secondary batteries are investigated by various analytical techniques.

2. Experimental

A Si–Zn–C composite was prepared by the following procedure. Commercial powders of Si (>99%, 2 μm, Kojundo) and Zn (>99%, 7 μm, Kojundo) with a mass ratio of 1:1 were mixed by mechanical ball-milling at a rotation speed of 500 rpm. Preliminary tests showed that the optimum milling time required to obtain a homogenous dispersion of Zn and an improved contact between Si and Zn was 10 h. MCMB (10–28, Osaka gas Co.)

* Corresponding author. Tel.: +82 2 880 7226; fax: +82 2 885 9671.
E-mail address: hjsohn@snu.ac.kr (H.-J. Sohn).

0378-7753/$ – see front matter © 2007 Elsevier B.V. All rights reserved.
doi:10.1016/j.jpowsour.2007.01.096

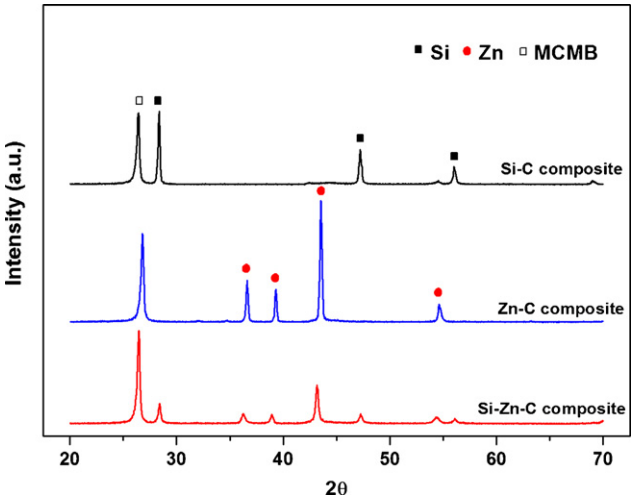

Fig. 1. X-ray diffraction patterns of powders synthesized by mechanical ball-milling.

was added to the mixed powders at a mass ratio of 2:1 and milled in an Ar-filled hardened steel vial at a rotation speed of 500 rpm for 1 h. The ball-to-powder ratio was 20:1. The final product was ground and particles with a mesh size of less than 200 were used. For comparison, Si and MCMB, as well as Zn and MCMB, with mass ratios of 1:2 were prepared by the same method. Each sample was characterized by X-ray diffraction (XRD; MacScience M18XHF-SRA). The morphology, microstructure and composition of the synthesized powders were examined by scanning electron microscopy (SEM) in conjunction with electron probe X-ray microanalysis (JEOL JXA-8900R).

The test electrodes consisted of the active powder material (70 wt.%), carbon black (15 wt.%) as a conducting agent and polyvinylidene fluoride (PVdF) dissolved in *N*-methyl pyrrolidinone (NMP) as a binder. Each component was well-mixed to form a slurry, which was coated on a foil copper foil and then subjected to pressing and drying at 120 °C for 4 h under vacuum. A coin-type electrochemical cell was used with lithium foil as a counter electrode and 1 M $LiPF_6$ in ethylene carbonate (EC)/diethylene carbonate (DEC) (1:1, v/v, Cheil Industries Inc.) as an electrolyte. The cell was assembled and all of the electrochemical tests were carried out in an Ar-filled glove-box. The charge–discharge experiments were performed galvanostatically within the voltage range of 0.05–1.5 V (versus Li/Li^+). The lower voltage limit was used to improve the cycling performance in the fully amorphous Si phase range [1] and to avoid the formation of metallic Li which might give rise to a safety hazard.

3. Results and discussion

The XRD patterns of the composite materials synthesized by mechanical ball-milling are shown in Fig. 1. All of the diffraction peaks are indexed to Si, Zn and graphite in good agreement with JCPDS data [15–17]. The decrease in the intensity of the peaks for Si and Zn in the case of the Si–Zn–C composite is a result of the two-step mechanical ball-milling process.

A scanning election micrograph of the agglomerates embedded in an epoxy resin and the corresponding electron probe X-ray microanalyses (EPMA) of the cross-sections of the Si–Zn–C composite material are shown in Fig. 2. The size of the agglom-

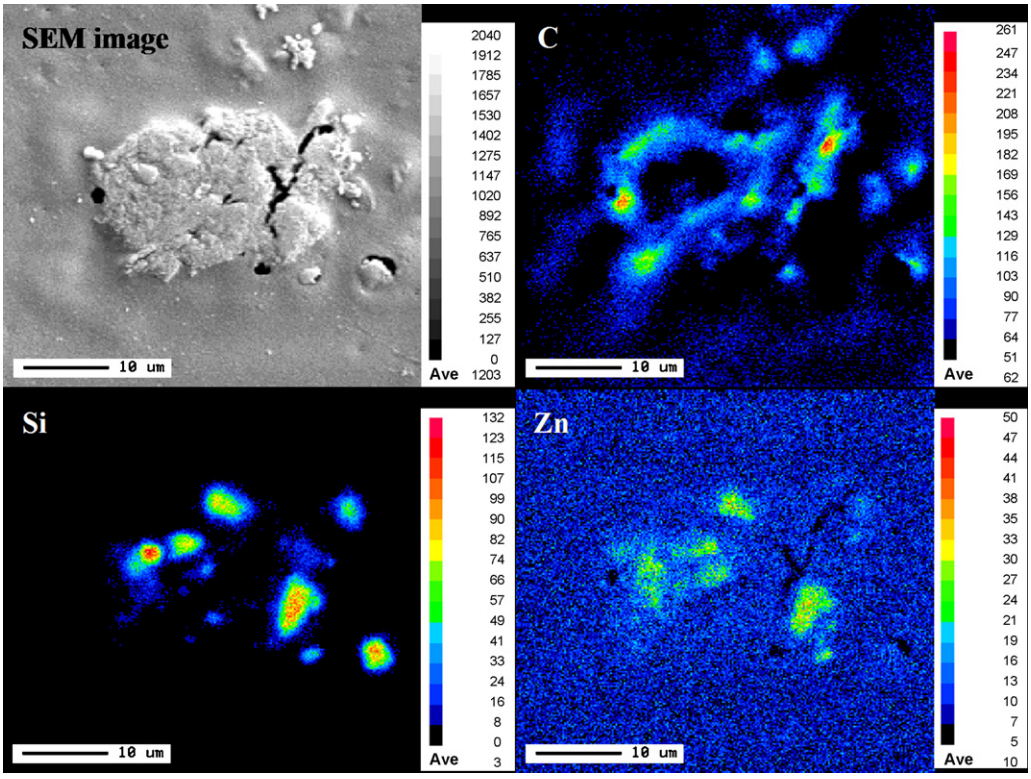

Fig. 2. Scanning electron micrograph and corresponding EPMA mapping of Si–Zn–C composite powder of agglomerates.

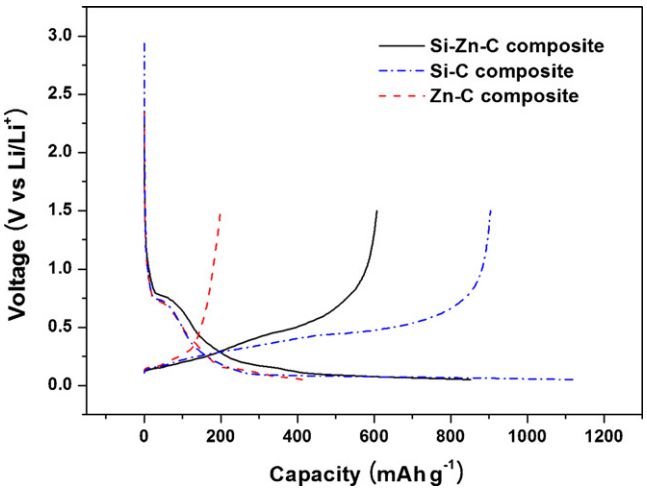

Fig. 3. Voltage profiles of Si–C, Zn–C and Si–Zn–C composites for first cycle.

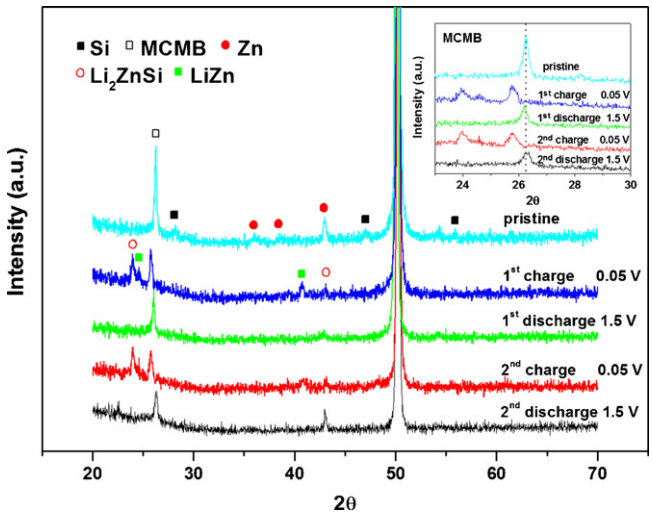

Fig. 4. Ex situ XRD data of Si–Zn–C composite electrode for first and second cycles.

erates is about 10–30 μm. As shown in the EPMA images, the Zn and Si particles appear together at nearby locations and are surrounded by graphite on the outside. This encapsulation would provide good electrical contact with the current-collector, as well as having a buffering effect on volume expansion–contraction during cycling.

The voltage profiles of the first charge–discharge curves of the Zn–C, Si–C and Si–Zn–C composite electrodes are given in Fig. 3 and were obtained at a constant current of 100 mA g^{-1} over the voltage range of 0.05–1.5 V (versus Li/Li^+). During the first cycle, charge (Li insertion), the electrolyte decomposes at approximately 0.75 V to form a solid electrolyte interface (SEI) [18] at the surface of the respective composite material. The first charge and discharge capacities of the Si–C composite are approximately 1118 and 903 mAh g^{-1}, respectively, which shows an initial cycling efficiency of 81%. The alloying reaction with lithium is observed as a flat plateau region below 0.1 V. The SEI and disordered graphite formed during milling are the main causes of the irreversible capacity of this composite. Compared with the Si–C composite electrode, the first charge and discharge capacities of the Zn–C composite are much lower, namely, 417 and 199 mAh g^{-1}, respectively, with an initial cycling efficiency of only 48%. Zinc has a relatively low theoretical specific capacity of 410 mAh g^{-1} for LiZn and its large irreversible capacity is mainly associated with the irreversible reaction between LiZn and the intermediate Li_2Zn_5 phase [19]. The irreversible capacity of the Si–Zn–C composite electrode is related to the properties of the Si–C and Zn–C composite electrodes, as discussed above, and the first charge and discharge capacities of the Si–Zn–C composite are 852 and 607 mAh g^{-1}, respectively, with an initial cycling efficiency of 71%.

The ex situ X-ray diffraction patterns of the Si–Zn–C composite electrodes are presented in Fig. 4. During the first charge, the Si peaks disappear because the crystalline Si phase changes into an amorphous counterpart by alloying with lithium [1,2,7]. Also, both binary LiZn and ternary Li_2ZnSi phases are observed, as shown by XRD data in Fig. 4. Lithium intercalation/de-intercalation into MCMB can also be identified through the low-angle shift, as shown in the inset of Fig. 4. The Li_2ZnSi ternary phase forms in the interface between Si and Zn during charging (Li insertion). Li_2ZnSi is a member of the M_2AX phases (where M is an early transition metal, A is an A group element and X is C or N). The M_2AX phases are generally good thermal and electrical conductors and exhibit a high elastic modulus, but they are readily machineable and relatively soft [13]. The Li_2ZnSi phase has a layered structure with Si and Zn forming layers between which the Li ions are located ($P\bar{3}m1$). Thus, the material allows lithium to move easily in and out of the structure [13,14,20]. After the first discharge, the Si and Li_2ZnSi phases disappeared, but the Zn and graphite phases reappear. The reactions of the Zn, Li_2ZnSi and graphite with Li during the second charge–discharge are similar to those observed during the first cycle.

A comparison of the cycle performances of the Zn–C, Si–C and Si–Zn–C composite electrodes is shown in Fig. 5 as a function of the cycle number. All of the electrodes were tested within a voltage window of 0.05–1.5 V (versus Li/Li^+) at a constant

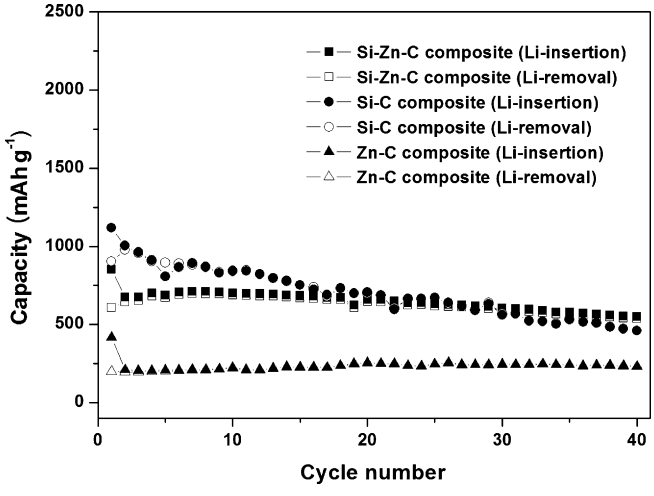

Fig. 5. Cycle performance of Si–C, Zn–C and Si–Zn–C composite electrode.

current of 100 mA g^{-1}, as mentioned previously. The Zn–C composite electrode shows stable capacity retention, due to its relatively small volume change of 70%, except for the large irreversible capacity during the first cycle. On the other hand, the Si–C composite electrode reveals continuous capacity fading, even though graphite is used to improve the electrical contact and alleviate the large volume change for Si (323%) during cycling. A relatively high reversible capacity and improved cycle performance can be observed for the Si–Zn–C composite, and 91% of its initial capacity of 607 mAh g^{-1} is retained after 40 cycles. This enhancement of capacity retention of Si–Zn–C composite electrode is probably due to the synergistic effect obtained by employing the third element, Zn, to form Li_2ZnSi in the interface between Si and Zn during charging.

4. Conclusions

A Si–Zn–C composite material was prepared by mechanical ball-milling. The Zn particles were uniformly blended with the Si particles and encircled by the graphite. Examination of the cycle-life performance of this composite material reveals that 91% of the initial discharge capacity of 607 mAh g^{-1} can be maintained for up to 40 cycles. The superior cycling performance of the composite electrode is attributed to buffering of the mechanical stress generated during cycling and to improved electrical connection with the current-collector afforded by the synergistic effect between Li_2ZnSi, Zn and graphite.

Acknowledgement

This work was supported by the Korea Science and Engineering Foundation (KOSEF) through the Research Center for Energy Conversion and Storage at Seoul National University (Grant No. R11-2002-102-00000-0).

References

[1] M.N. Obrovac, L. Christensen, Electrochem. Solid-State Lett. 7 (2004) A93.
[2] T.D. Hatchard, J.R. Dahn, J. Electrochem. Soc. 151 (2004) A838.
[3] I.-S. Kim, P.N. Kumta, G.E. Blomgren, Electrochem. Solid-State Lett. 3 (2000) 493.
[4] I.-S. Kim, G.E. Blomgren, P.N. Kumta, Electrochem. Solid-State Lett. 6 (2003) A157.
[5] J.-H. Kim, H. Kim, H.-J. Sohn, Elctrochem. Commun. 7 (2005) 557.
[6] S. Yoon, S.-I. Lee, H. Kim, H.-J. Sohn, J. Power Sources 161 (2006) 1319.
[7] M.-S. Park, Y.-J. Lee, S. Rajendran, M.-S. Song, H.-S. Kim, J.-Y. Lee, Electrochim. Acta 50 (2005) 5561.
[8] H.-Y. Lee, S.-M. Lee, Elctrochem. Commun. 6 (2004) 465.
[9] Y. Liu, K. Hanai, J. Yang, N. Imanishi, A. Hirano, Y. Takeda, Electrochem. Solid-State Lett. 7 (2004) A369.
[10] Y. Liu, K.T. Matsumura, N. Imanishi, A. Hirano, T. Ichikawa, Y. Takeda, Electrochem. Solid-State Lett. 8 (2005) A599.
[11] J. Yang, B.F. Wang, K. Wang, Y. Liu, J.Y. Xie, Z.S. Wen, Electrochem. Solid-State Lett. 6 (2003) A154.
[12] M. Yoshio, H. Wang, K. Fukuda, T. Umeno, N. Dimov, Z. Ogumi, J. Electrochem. Soc. 149 (2002) A1598.
[13] T.D. Hatchard, M.N. Obrovac, J.R. Dahn, J. Electrochem. Soc. 152 (2005) A2335.
[14] T.D. Hatchard, M.N. Obrovac, J.R. Dahn, J. Electrochem. Soc. 153 (2006) A282.
[15] JCPDS, file no. 80-0018.
[16] JCPDS, file no. 87-0713.
[17] JCPDS, file no. 75-2078.
[18] E. Peled, J. Electrochem. Soc. 126 (1979) 2047.
[19] T. Fujieda, S. Takahashi, S. Higuchi, J. Power Sources 40 (1992) 283.
[20] Z. Sun, D. Music, R. Ahuja, J.M. Schneider, J. Appl. Phys. 99 (2006) 053509.